Ligand Preorganization in Metal Ion Complexation: Molecular Mechanics/Dynamics, Kinetics, and Laser-Excited Luminescence Studies of Trivalent Lanthanide Complex Formation with Macrocyclic Ligands TETA and DOTA

C. Allen Chang,*,† Yuh-Liang Liu,† Chang-Yuh Chen,† and Xiu-Mei Chou‡

Department of Biological Science and Technology, National Chiao Tung University, Hsinchu, Taiwan, and National Center for High-Performance Computing, National Science Council, Hsinchu, Taiwan

Received November 28, 2000

The molecular mechanics and dynamics calculations, kinetics, and laser-excited luminescence studies were carried out for trivalent lanthanide (Ln^{3+}) complexes of macrocyclic polyaminopolycarboxylate ligands TETA and DOTA (where TETA is 1,4,8,11-tetraazacyclotetradecane-1,4,8,11-tetraacetic acid and DOTA is 1,4,7,10-tetraazacyclododecane-1,4,7,10-tetraacetic acid) to further understand the observed thermodynamic, kinetic, and structural properties and to examine how ligand preorganization affects metal ion complexation. Excitation spectroscopy (emission monitored at 614.0 nm) of the $^7F_0 \rightarrow {}^5D_0$ transition of Eu^{3+} was used to study the aqueous properties of the Eu^{3+}−TETA system. A stopped-flow spectrophotometric method was used to study the formation kinetics of the aqueous Ce^{3+}−TETA/DOTA systems in the pH range 6.1−6.7. Molecular mechanics calculation results are consistent with the proposed mechanism of $Ln(DOTA)^-$ formation, i.e., formation of a carboxylate O-bonded precursor, followed by metal ion moving into the preformed macrocyclic cavity. For $Ln(TETA)^-$ formation, at least two carboxylate O-bonded intermediates have been predicted and Ln^{3+} ion assisted reorganization of the TETA ligand is present. The calculated bond distances and overall structures of $Ln(DOTA)^-$ and $Ln(TETA)^-$ were in agreement with the single-crystal and solution NMR structural data. The origin of the difference in thermodynamic stability of $Ln(DOTA)^-$ and $Ln(TETA)^-$ complexes and the corresponding formation intermediates is mainly due to the differences in water-occupancy energy (i.e., whether there is an apical coordinated water molecule), the ligand strain energy, and the cation−ligand interaction energy. Kinetic studies revealed that the formation rates of the $Ce(TETA)^-$ complex are smaller at lower pH and temperature but become greater at higher pH and temperature, as compared to those of the $Ce(DOTA)^-$ complex. This is attributed to the lanthanide ion and both mono- and di-hydroxide ion assisted TETA conformational reorganization and higher kinetic activation parameters. The presence of a di-hydroxide ion assisted intermediate rearrangement pathway could make the $Ce(TETA)^-$ complex formation rate faster at higher pH, and the higher activation barrier makes $Ce(TETA)^-$ complex formation rate slower at lower pH, as compared to those of the $Ce(DOTA)^-$ complex.

Introduction

Ligand preorganization is the tendency of free ligand to assume the conformation necessary for metal ion complexation which results in increased metal complex stability.[1] There are many cases of ligand/protein preorganization found in coordination chemistry and metallo-biochemistry. For example, the first preorganized siderophore (microbial iron transport agent) alcaligin has a macrocyclic structure, and it forms a more stable Fe(III) complex than the noncyclic, nonpreorganized rhodotorulic acid.[2] Chelating agents with a *trans*-cyclohexylenediamine backbone such as *trans*-cyclohexyldiamine tetraacetic acid (CDTA) and structural analogues tend to form more stable complexes than do EDTA and analogues;[3,4] and the former are preferred to be used for imaging and radiotherapeutic purposes.

In the search for stable, safe, and efficacious agents for use as magnetic imaging contrast agents and artificial DNA/RNA cleavage agents, it has been demonstrated that, for trivalent lanthanide (Ln^{3+}) complexes of rigid macrocyclic (12-membered ring) polyaminopolycarboxylate ligands such as DOTA (1,4,7,10-tetraazacyclododecane-1,4,7,10-tetraacetic acid) and HPDO3A (10-(2-hydroxypropyl)-1,4,7,10- tetraazacyclododecane), stability and kinetic inertia increase with increasing charge density of the metal ion and are normally greater than those of the linear ligands such as DTPA (diethylenetriaminepentaacetic acid).[5−9] On the other hand, lanthanide complexes with the 14-membered-ring structural analogue, TETA (1,4,8,11-tetraazacyclotetradecane-1,4,8,11-tetraacetic acid), have quite different coordination properties. For example, the stability constant of $Gd(TETA)^-$, $\log K_f = 14.7$,[10] is about 10 log K units lower than that of

† National Chiao Tung University.
‡ National Science Council.

(1) Hancock, R. D.; Martell, A. E. *Chem. Rev.* **1989**, *89*, 1875.
(2) Hou, Z.; Sunderland, C. J.; Nishio, T.; Raymond, K. N. *J. Am. Chem. Soc.* **1996**, *118*, 5148−5149.
(3) Schwarzenbach, G.; Gut, R.; Anderegg, G. *Helv. Chim. Acta* **1954**, *37*, 937.
(4) Brechbiel, M. W.; Gansow, O. A.; Pippin, C. G.; Rogers, R. D.; Planalp, R. P. *Inorg. Chem.* **1996**, *35*, 6343−6348.
(5) Cacheris, W. P.; Nickle, S. K.; Sherry, A. D. *Inorg. Chem.* **1987**, *26*, 958−960.
(6) Kodama, M.; Koike, T.; Mahatma, B.; Kimura, E. *Inorg. Chem.* **1991**, *30*, 1270−1273.
(7) Kumar, K.; Tweedle, M. F. *Inorg. Chem.* **1993**, *32*, 4193−4199.
(8) Toth, E.; Brucher, E.; Lazar, I.; Toth, I. *Inorg. Chem.* **1994**, *33*, 4070−4076.
(9) Wu, S. L.; Horrocks, W. D. *Inorg. Chem.* **1995**, *34*, 3724−3732.
(10) Kumar, K.; Chang, C. A.; Francesconi, L. C.; Dischino, D. D.; Malley, M. F.; Gougoutas, J. Z.; Tweedle, M. F. *Inorg. Chem.* **1994**, *33*, 3567−3575.

10.1021/ic001325j CCC: $20.00
Published on Web 05/26/2001

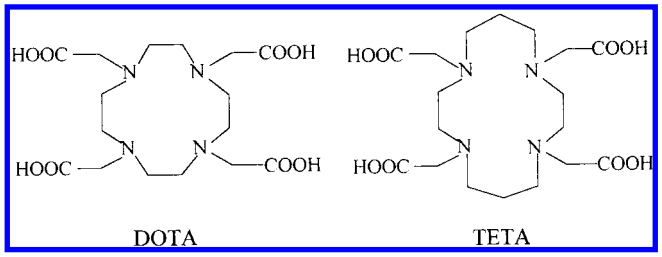

Figure 1. Structural formulas of 1,4,7,10-tetraazacyclododecane-1,4,7,10-tetraacetic acid (DOTA) and 1,4,8,11-tetraazacyclotetradecane-1,4,8,11-tetraacetic acid (TETA).

$Gd(DOTA)^-$, log $K_f = 25.3$.[6] Kinetically, both $Ln(DOTA)^-$ and $Ln(TETA)^-$ are slow to form and dissociate[7,8] as compared to the lanthanide complexes of linear ligands such as EDTA and DTPA.[11] However, the proton-catalyzed dissociation rates are much faster for $Ce(TETA)^-$ than for $Ce(DOTA)^-$. In particular, the rate difference between $Ce(DOTA)^-$ and $Ce(TETA)^-$ for the monoprotonated complex dissociation pathway is mainly due to the difference in $\Delta H^{\ddagger}$.[12] Figure 1 shows the structural formulas of DOTA and TETA.

Crystal structures of Gd(III) and Y(III) complexes of DOTA and HPDO3A indicated that these complexes are nine-coordinated. The metal ions are eight- coordinated by the ligand (i.e., four nitrogen and four oxygen atoms), with a water molecule occupying the ninth (apical) position.[13,14] The structures of the free and complexed ligand DOTA are similar, i.e., all four carboxylate pendent groups have a syn configuration with respect to the plane formed by the four nitrogen atoms.[10] This indicates that only limited DOTA ligand reorganization is needed for metal ion complexation, i.e., DOTA has a preorganized structure. On the other hand, the two pairs of adjacent carboxymethyl groups of the structurally similar ligand TETA take the anti configuration.[15] Upon metal ion complexation, the TETA ligand conformation is drastically rearranged so that the four carboxymethyl groups are in the syn configuration.[16] Both diamagnetic and paramagnetic NMR studies of lanthanide complexes of DOTA and TETA indicated that these complexes have very rigid structures in aqueous solution.[17−19] Computer-simulated structures are also consistent with those found in the solid state.[20]

It has been postulated that the preorganized ligands such as DOTA form more stable and inert lanthanide complexes than those without, such as TETA. Although a number of studies have been reported for $Ln(DOTA)^-$ complexes, few have been for $Ln(TETA)^-$ complexes. In particular, $Ln(TETA)^-$ complex formation kinetics has not been reported. Thus, the present studies are performed for (1) the general understanding of thermodynamic (stability and selectivity), kinetic (lability), and structural properties of lanthanide(III) aminopolycarboxylate ligands; (2) the determination of possible lanthanide−DOTA/TETA complexation mechanisms and potential reaction intermediates; (3) the determination of possible structures of the reaction intermediates and final products; (4) the determination of possible energetics of the complexation reactions; (5) the understanding of relationships of results of molecular mechanics studies with thermodynamic, kinetic, and structural characterizations; (6) applications as magnetic resonance imaging (MRI) contrast enhancement agents, molecular luminescence probes, and DNA/RNA cleavage agents.

Table 1. Force-Field Parameters

atom	CHARMm type	partial charge	*R*(min)	*e*(min)
carboxylate charged O	OT	−0.65[a]	1.550	−0.1521
carboxylate carbonyl O	OAC	−0.55[a]	1.520	−0.1591
amine N	NT	−0.4	1.650	−0.1500
Eu	MEU	3.0	1.800	−0.2000
water O (TIP3)	OW	−0.834	1.768	−0.1521

[a] It was necessary to differentiate between the two carboxylate oxygen atoms to avoid a strong preference toward bidentate coordination during energy minimization.

Experimental Section

Materials. Reagent grade potassium chloride, cerium nitrate, and europium nitrate were used as received. The ligands were synthesized and purified according to the reported methods.[10,17] Aqueous solutions of the ligands were prepared by weight and standardized by potentiometric and complexometric titrations with standardized HCl and cerium nitrate solutions, respectively.[21,22] Standard solutions of Ce^{3+} and Eu^{3+} were prepared from cerium and europium nitrate and standardized by EDTA titrations, respectively. KCl was used to adjust the ionic strength. All solutions were prepared using deionized water.

Molecular mechanics and molecular dynamics calculations were carried out according to published procedures with minor modifications.[20] A Silicon Graphics Workstation (CPU model R4400) with a Silicon Graphics Power Challenge (CPU model R8000) system and the Quanta 4.1 Molecular Graphics Package and the CHARMm 2.3 Molecular Mechanics/Dynamics program were used. Force-field parameters are listed in Table 1. Energy minimization was carried out using a conjugated-gradient method with a convergence criterion of 0.01 kcal/mol. Molecular dynamics calculations were carried out using the Verlet algorithm to integrate Newton's equation with time step of 1.0 fs.

Laser-Excited Eu^{3+} Luminescence Measurements. Laser-excited luminescence experiments were performed at the Regional Instrument Center of National Science Council located at the Chemistry Department, National Tsing Hwa University, Hsinchu, Taiwan.[23] A Spectra Physics PDL3 dye laser was employed using a mixture of R590 and R610 dyes. The ratio of the two dyes was adjusted to ensure that the lasing power throughout the scanning region remained constant. A Spectra Physics DCR2A Nd:YAG laser, using its second harmonic line (532 nm), pumped the dye laser. The output power of the laser was 85−90 mJ/pulse. The excitation spectra were obtained by scanning between 577 and 581 nm at a rate of 0.02 nm/step. The emission was focused into a Jobin Yvon HR320 monochromator equipped with a Hammatsu R980 photomultiplier. The high voltage for the PMT was supplied by a Stanford Research PS325 power supply. An R610 filter was placed in front of the monochromator to eliminate laser scatter. The electronic signal was averaged by a boxcar averager constructed with a Stanford Research SR245 interface, an SR250 gate integrator, and an SR280 mainframe and power. A program written in ASYST and run on a 486SX microcomputer controlled the system. Emission decay curves were recorded on a LeCroy 9450 oscilloscope. The average of 1000 decay curves was reported.

(11) Nyssen, G. A.; Margerum, D. W. *Inorg. Chem.* **1970**, *9*, 1814−1820.
(12) Chang, C. A.; Liu, Y. L. *J. Chin. Chem. Soc.* **2000**, *47*, 1001−1006.
(13) Chang, C. A.; Francesconi, L. C.; Malley, M. F.; Kumar, K.; Gougoutas, J. Z.; Tweedle, M. F.; Lee, D. W.; Wilson, L. J. *Inorg. Chem.* **1993**, *32*, 3501−3508.
(14) Spirlet, M.-R.; Rebizant, J.; Desreux, J. F.; Loncin, M.-F. *Inorg. Chem.* **1984**, *23*, 359−363.
(15) Maurya, M. R.; Zaluzec, E. J.; Pavkovic, S. F.; Herlinger, A. W. *Inorg. Chem.* **1991**, *30*, 3657−3662.
(16) Spirlet, M.-R.; Rebizant, J.; Loncin, M.-F.; Desreux, J. F. *Inorg. Chem.* **1984**, 23, 4278−4283.
(17) Desreux, J. F. *Inorg. Chem.* **1980**, *19*, 1319−1324.
(18) Desreux, J. F.; Loncin, M. F. *Inorg. Chem.* **1986**, *25*, 69−74.
(19) Jacques, V.; Desreux, J. F. *Inorg. Chem.* **1994**, *33*, 4048−4053.
(20) Fossheim, R.; Dahl, S. D. *Acta Chem. Scand.* **1990**, *44*, 698−706.
(21) Sekhar, V. C.; Chang, C. A. *Inorg. Chem.* **1986**, *25*, 2061−2065.
(22) Chang, C. A.; Sekhar, V. C. *Inorg. Chem.* **1987**, *26*, 1981−1985.
(23) Chang, C. A.; Chen, Y. H.; Chen, H. Y.; Shieh, F. K. *J. Chem. Soc., Dalton Trans.* **1998**, 3243−3248.

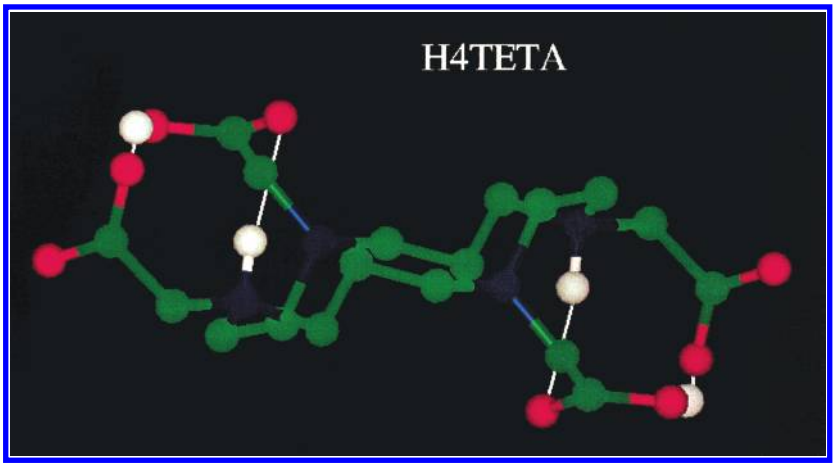

Figure 2. Molecular mechanics calculated structure of H_4TETA. The structure takes an anti configuration with two intramolecular H-bonds.

Before new data were obtained, the laser-excited luminescence measurements were performed on Eu^{3+}−EDTA/DTPA systems (pH 5.2). The excitation spectral maxima obtained for Eu^{3+} (578.68 nm), Eu^{3+}−EDTA (579.57 and 580.05 nm), and Eu^{3+}−DTPA (579.88 nm) were consistent with literature reported findings.[24] The respective Eu^{3+} and TETA solution concentrations were prepared to be 0.200 and 0.204 mM (the slight excess of TETA at pH 6.10 is to minimize the concentration of free Eu^{3+} ion). The ionic strength was adjusted to 0.1 using 1 M $(CH_3)_4NCl$ solution. Control of buffer pH was achieved using buffer reagents, MES (pH 5 0−7.0), HEPES (pH 7.0−9.0), and CAPS (pH 9.0−11.0).

Kinetic Measurements. Spectra and slower kinetic runs were made with a Hewlett-Packard 8453 diode-array spectrophotometer equipped with a thermostated cell holder. A stopped-flow spectrophotometer (Photal-Otsuka Electronics, RA-401) was used for faster kinetic runs. The reactions were initiated by mixing equal volumes of solutions of cerium nitrate (final concentrations 2.0−5.0 mM) with the buffered ligand solutions (final concentration 0.2 mM, pH 6.1−6.7). Reactions were monitored by recording absorbance changes at 295 nm $(CeTETA)^-$ and 320 nm $(CeDOTA)^-$. The temperature of the observation cell was maintained at 25.0, 32.0, 39.0, and 45.0 °C (±0.1 °C). All reactions were pseudo-first-order, and the observed rate constants, k_{obs}, were obtained using standard least-squares procedures to fit the data to the expression

$$A_t = A_\infty + (A_0 - A_\infty)\exp(-k_{obs}t) \quad (1)$$

where A_t, A_0, and A_∞ are the instantaneous, initial, and final absorbance values, respectively. Each value of k_{obs} reported represents the average of four to six replicate runs. The relative error for most data is less than 5%. Other experimental conditions were as follows: ionic strength = 1.0 M, KCl; mixing pressure 5 kg/cm^2, N_2 gas.

Results and Discussion

Molecular Mechanics Calculated Structures, Stability, and Energy of the Ln(III)−DOTA/TETA Complexes and Potential Intermediates. The calculated free ligand structures of H_6DOTA^{2+} and H_2DOTA^{2-} (Figure S1, Supporting Information) have very similar backbone conformations, i.e., all four carboxymethyl groups point to the same direction relative to the plane formed by the four nitrogen atoms of the macrocyclic ring and maintain a syn configuration. This is consistent with the result of the free DOTA ligand reported by a previous paper.[10] The calculated structure of H_4TETA reveals that two pairs of carboxymethyl groups separated by trimethylene units adopt an anti configuration (Figure 2). Two hydrogen bonds are present with each pair of carboxymethyl groups: one between the carboxylic acid and the carboxylate groups, the other between a carboxylate and the protonated ring nitrogen groups. This structure is slightly different from the crystal structure of $H_4TETA\cdot 4H_2O$ reported earlier in which the hydrogen-bonding pattern is complex.[15]

Calculations of the final Ln(III)−DOTA/TETA complex structures have assumed the parameters of Eu(III) ion and which cannot be distinguished from most of the other lanthanide ions. Table 2 lists the reaction energy in vacuo and in aqueous environment, constraint energy of ligand by complexation, ligand−ion interaction energy, and hydration energy for both Eu(III)−DOTA/TETA complexes. From the complexation reaction mechanistic point of view (vide infra), the energies associated with potential intermediates, Eu(III)−H_2DOTA/H_2-TETA, have also been calculated and are listed in Table 2. The bond distances of the energy-minimized Eu(III)−DOTA/TETA and Eu(III)−H_2DOTA/H_2TETA structures are listed in Table 3.

Table 2. Total Energy, Constraint Energy of Ligand by Complexation, Ligand−Ion Interaction Energy, and Mono- and Di-hydrogen Energies of Ln(III)−DOTA/TETA Complexes (kcal/mole)

	$E_{R,g}$	$E_{D,L}$	E_I	E_{H1}	E_{H2}	$E_{R,aq}$
$Eu(H_2DOTA)^+$	−348.8	61.4	−410.2	48.9	−198.9	−498.8
$Eu(H_2TETA)^+$	−337.3	151.4	−488.6	64.7	−143.2	−415.8
$Eu(DOTA)^-$	−501.5	88.7	−590.2	151.4	− 34.4	−384.7
$Eu(TETA)^-$	−456.7	98.7	−555.3	158.7	− 5.2	−303.1

$E_{R,g} = E_{ML} - E_L = E_I + E_{D,L}$ ($E_{ML} = E_I + E_{LC}$; $E_{D,L} = E_{LC} - E_L$)
$E_{H1} = E_{H,ML} - E_{H,L} + E_{H,W}$ ($E_{H,W} = -5.2n$)
$E_{H2} = E_{H,M} + E_{H,W}$
$E_{R,aq} = E_{R,g} + E_{H1} + E_{H2}$ = reaction energy in aqueous environment
$E_{R,g}$ = reaction energy of complexation in vacuo
E_{ML} = total energy of the cation−ligand complex
E_L = energy of the lowest energy conformer of the free ligand
E_I = interaction energy between cation and ligand
$E_{D,L}$ = constraint energy of the ligand in the complex
E_{LC} = energy of the ligand in the complex
E_{H1} = energy difference between hydration of carboxylate groups in free ligands and in complexes
$E_{H,ML}$ = the interaction energy between water molecules H-bonded to uncoordinated carboxylate groups in complexes (ML)
$E_{H,L}$ = the interaction energy between water molecules H-bonded to uncoordinated carboxylate groups in ligands (L)
$E_{H,W}$ = the water−water interaction energy = $-5.2n$ (n = number of carboxylate-water H-bonds lost by complexation)
E_{H2} = the hydration energy of lanthanide ion in a complex by occupancy of vacant coordination sites
$E_{H,M}$ = the mono- or di-hydration energy of the complexes

(24) Wu, S. L.; Horrocks, W. D., Jr. *Anal. Chem.* **1996**, *68*, 394.

Table 3. Calculated Bond Distances of Ln(III)−DOTA/TETA Complexes (Å)

	bond distances					average
$Eu(H_2TETA)^+$						
Eu−O (carboxylate)	2.307	2.370	2.307	2.298		2.32
Eu−O (H_2O)	2.514	2.522	2.514			2.52
Eu−O plane						1.11
$Eu(TETA)^-$						
Eu−N	2.553	2.645	2.582	2.642		2.61 (2.60)[a]
Eu−O (carboxylate)	2.301	2.303	2.348	2.302		2.31 (2.31)[a]
Eu−O (H_2O)						
Eu−O plane						1.16 (1.21)[a]
Eu−N plane						1.15 (1.25)[a]
$Eu(H_2DOTA)^+$						
Eu−O (carboxylate)	2.349	2.323	2.340	2.363		2.34
Eu−O (H_2O)	2.594	2.537	2.575	2.551	2.617	2.57
Eu−O plane						
$Eu(DOTA)^-$						
Eu−N		2.548	2.632	2.595	2.567	2.59 (2.66)[b]
Eu−O (carboxylate)	2.329	2.327	2.324	2.350		2.33 (2.37)[b]
Eu−O (H_2O)	2.557					2.56 (2.46)[b]
Eu−O plane						0.79 (0.72)[b]
Eu−N plane						1.50 (1.63)[b]

[a] Reference 16. [b] Reference 13.

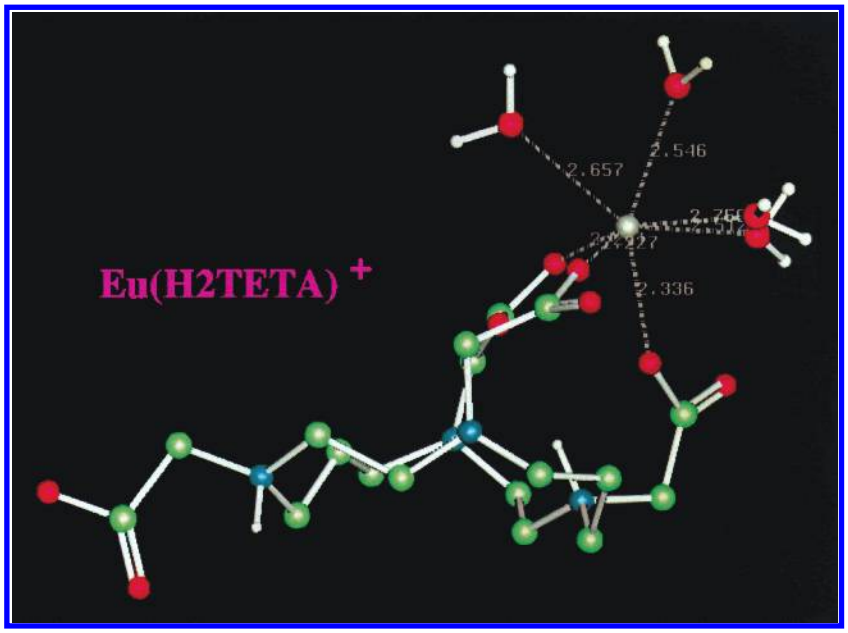

Figure 3. One potential Eu(III)−H_2TETA intermediate structure. The Eu(III) ion is coordinated to three carboxylate groups in the syn configuration.

Both calculated $Eu(DOTA)^-$ and $Eu(TETA)^-$ structures are very similar to their corresponding single-crystal structures (Figures S2 and S3, Supporting Information). The calculated Eu−O and Eu−N average bond distances are almost the same as those of the crystal structures with only minor differences. $Eu(DOTA)^-$ is nine-coordinated, eight with the ligand; the ninth (apical) position is occupied by a water molecule. The coordinated DOTA ligand structure is similar to that of the free form and, therefore, is preorganized for complexation. On the other hand, the coordinated TETA ligand in $Eu(TETA)^-$ has been rearranged to take a syn configuration and all four carboxymethyl groups point toward the same direction defined by the four nitrogen atoms. The $Eu(TETA)^-$ is only eight-coordinated by the ligand without apical water coordination because the 14-membered ring has a larger cavity size and the lanthanide ion is deeper in the pocket. This is illustrated by the shorter Eu−N plane distance, i.e., 1.15 Å of $Eu(TETA)^-$ as compared to that of $Eu(DOTA)^-$, i.e., 1.50 Å.

The intermediate, Eu(III)−H_2DOTA, has been directly observed by luminescence spectroscopic means, and the molecular mechanics calculation predicted a structure involving coordination of Eu(III) ion to the four carboxylate groups well away from the plane of the four nitrogen atoms.[9] However, for the Eu(III)−H_2TETA system, in addition to the similar four-carboxylate bound syn structural intermediate (Figure S4, Supporting Information), another interesting structure is also predicted, in which the Eu(III) ion is coordinated to three carboxylate groups in the syn configuration with the remaining coordination sites occupied by water molecules (Figure 3). Although this structure could later turn into the four-carboxylate coordinated syn intermediate, it indicates that the presence of Eu(III) ion could induce the TETA ligand conformation rearrangement for metal ion complexation (vide infra).

As expected, the calculations predict that the complex stability decreases in the order $Eu(DOTA)^-$ > $Eu(TETA)^-$ and $Eu(H_2DOTA)^+$ > $Eu(H_2TETA)^+$. It is interesting to observe that,

Scheme 1. Possible Complexation Reaction Mechanisms

DOTA :

$$Ln(H_2O)_m^{3+} + H_nDOTA^{(n-4)+} \leftrightarrow Ln(H_2DOTA)(H_2O)_{m-4}^{+,*} + 4H_2O + (n-2)H^+$$

pre-organized, ***syn*** 4 -COO^- coordinated species

$$Ln(H_2DOTA)(H_2O)_{m-4}^{+,*} \rightarrow Ln(DOTA)(H_2O)^- + (m-5)H_2O \qquad m = 8 \text{ or } 9$$

TETA :

$$Ln(H_2O)_m^{3+} + H_nTETA^{(n-4)+} \leftrightarrow Ln(H_2TETA)(H_2O)_{m-3}^{+,*} + 3H_2O + (n-2)H^+$$

not pre-organized, ***anti*** 3 -COO^- coordinated species

$$Ln(H_2TETA)(H_2O)_{m-3}^{+,*} \leftrightarrow Ln(H_2TETA)(H_2O)_{m-4}^{+,**} + H_2O$$

4 -COO^- coordinated species

$$Ln(H_2TETA)(H_2O)_{m-4}^{+,**} \rightarrow Ln(TETA)^- + (m-4)H_2O \qquad m = 8 \text{ or } 9$$

except for the cation−ligand interaction energy, all other energies favor both intermediate and final $Ln(DOTA)^-$ complex formation, including the water-occupancy energy (i.e., whether there is an apical coordinated water molecule) and the ligand constraint energy. Previously, it has been calculated that the more flexible ligand DTPA has greater ligand constraint energy than that of DOTA.[20] Similarly, the TETA ligand with larger macrocyclic cavity could be considered more flexible than DOTA and, therefore, has greater ligand constraint energy. The less favored TETA ligand constraint energy and water occupancy energy are only partly compensated by the more favored cation−ligand interaction energy, resulting in an overall less stable intermediate and final $Ln(TETA)^-$ complex formation.

Possible Complexation Mechanisms. Molecular dynamics simulations showed that the $Eu(DOTA)^-$ complex formation mechanism is consistent with what has been proposed by kinetic studies which involves the formation of an intermediate (e.g., Eu(DOTA)*, the precursor) in an equilibrium step, followed by a base-assisted reorganization to form the final complex,[7−9] $Eu(DOTA)^-$ (Scheme 1). On the other hand, the kinetics of the $Eu(TETA)^-$ complex formation reaction has not been reported previously. Our current calculation results showed that complexation started with coordination of the Eu(III) ion to one or two adjacent carboxylate groups with concomitant loss of coordinated water molecules. This is followed by a cation-induced ligand conformation rearrangement so that the Eu(III) ion coordinated to three syn carboxylate groups and later four. The final complex is formed by the Eu(III) ion moving into the TETA macrocycle cavity without any coordinated water molecule.

The kinetic implications of the molecular dynamics simulation study results could mean that the activation parameters of the $Eu(TETA)^-$ formation reaction might not be greater than those of the $Eu(DOTA)^-$ formation reaction because the nonpreorganized TETA ligand does not follow a concerted conformational change for metal ion complexation. Instead, the TETA ligand conformational change is a sequential event catalyzed by the presence of a metal ion (as well as a OH^- ion, vide infra), and this could result in faster formation reaction rates.

Laser-Excited Luminescence Studies. Laser excitation spectra of the transition of $^7F_0 \rightarrow {}^5D_0$ of Eu^{3+} solutions in the presence of ligand TETA could be used to deduce possible complexation intermediates and final product (excitation at 577−581 nm, emission at 614 nm, $^5D_0 \rightarrow {}^7F_2$). At different solution pH, this technique could be used as a preliminary check for further detailed kinetic studies. During the process of complexation, the initial association of Eu^{3+} with TETA and the final formation of $Eu(TETA)^-$ result in different ligand coordination fields and therefore different excitation spectra.

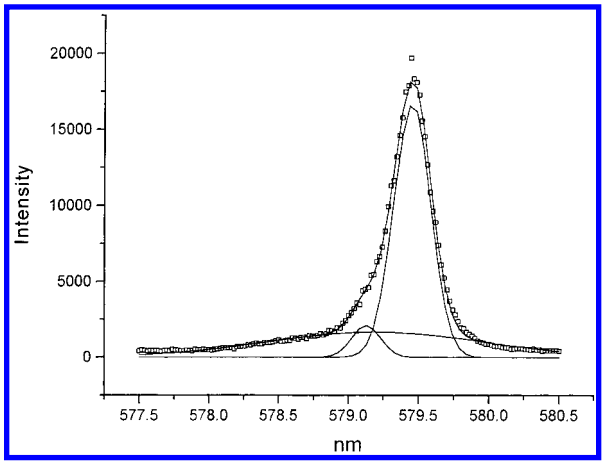

Figure 4. The excitation spectrum of $Eu(TETA)^-$, 0.2 mM, pH 6.1.

The complexation reaction between Eu^{3+} and TETA is tentatively proposed to involve the following three steps:

$$Eu^{3+} + H_2TETA^{2-} \leftrightarrow Eu(H_2TETA)^+ \xrightarrow{-H^+} Eu(HTETA) \xrightarrow{-H^+} EuTETA^- \quad (2)$$

The first step is a fast equilibrium; the second and/or the third deprotonation reaction is considered rate-determining.

Figure 4 shows the excitation spectrum of a 1:1, 0.2 mM Eu^{3+}/TETA solution mixture at pH 6.10. This spectrum was obtained within 15 min after sample preparation, and its profile and intensity did not change with time for 48 h. This indicated that the reaction reached equilibrium within 15 min after mixing. To verify this observation, the excitation spectra of a 1:1, 0.2 mM Eu^{3+}/TETA solution (pH 6.10) prepared and stored for 200 h and a solution freshly prepared by titrating a 1:1, 0.2 mM Eu^{3+}/TETA solution with $(CH_3)_4NOH$ to pH 9.90 were compared. The result showed that the two spectra are quite the same. Detailed analysis of the spectra indicates that there are two emission bands at 579.14 and 579.46 nm, and the intensity ratios of the two bands are roughly the same for all spectra measured at pH 6.10. The major peak at 579.46 nm is tentatively assigned to be from the final complex $Eu(TETA)^-$, and it is in line with the reported emission wavelengths of $Eu(DOTA)^-$ (579.77 nm) and $Eu(DTPA)^{2-}$ (579.88 nm). The origin of the small peak at 579.14 nm is not clear. Although the $Eu(DOTA)^-$ intermediate emission wavelength has been determined to be 579.20 nm[9] and it was mentioned in a paper[25] (cited as unpublished result) that a relatively stable $Eu(TETA)^-$ intermediate has been directly observed, we did not have concrete spectral evidence for the intermediate formation at pH 6.10 (i.e., the half-life of the intermediate is too short) and further study (perhaps at lower pH) is necessary.

Kinetic Studies. The studies were performed under pseudo-first-order reaction conditions: $[Ce^{3+}] \geq 10[TETA]$. Table 4 lists the obtained rate constants at four different temperatures

(25) Wu, S. L.; Johnson, K. A.; Horrocks, W. D., Jr. *Inorg. Chem.* **1997**, *36*, 1884−1889.

Table 4. Observed Rate Constants (k_{obs}, s^{-1}) for the Formation of Cerium(III)−TETA Complex at pH 6.1−6.7 at Four Different Temperatures, $\mu = 1.0$ (KCl)

		k_{obs}, s^{-1}			
pH	[Ce^{3+}], M	25 °C	32 °C	39 °C	45 °C
6.1	0.002		0.019	0.04	0.092
	0.0026		0.022	0.0466	0.106
	0.0032		0.0234	0.0499	0.111
	0.0038		0.0238	0.0503	0.114
	0.0044		0.0244	0.0516	0.116
	0.005		0.025	0.052	0.12
6.3	0.002	0.0154	0.0493	0.112	0.236
	0.0026	0.0179	0.0588	0.127	0.262
	0.0032	0.0184	0.0624	0.132	0.268
	0.0038	0.0195	0.064	0.137	0.279
	0.0044	0.0203	0.0648	0.141	0.285
	0.005	0.0217	0.0654	0.144	0.29
6.5	0.002	0.0325	0.091	0.22	0.452
	0.0026	0.0386	0.102	0.249	0.53
	0.0032	0.0408	0.111	0.268	0.566
	0.0038	0.0413	0.112	0.283	0.588
	0.0044	0.0429	0.116	0.296	0.597
	0.005	0.0434	0.118	0.3	0.605
6.7	0.002	0.0599	0.162	0.417	0.898
	0.0026	0.0728	0.198	0.494	1.014
	0.0032	0.0779	0.208	0.523	1.094
	0.0038	0.0832	0.216	0.546	1.11
	0.0044	0.084	0.224	0.555	1.115
	0.005	0.0852	0.228	0.58	1.127

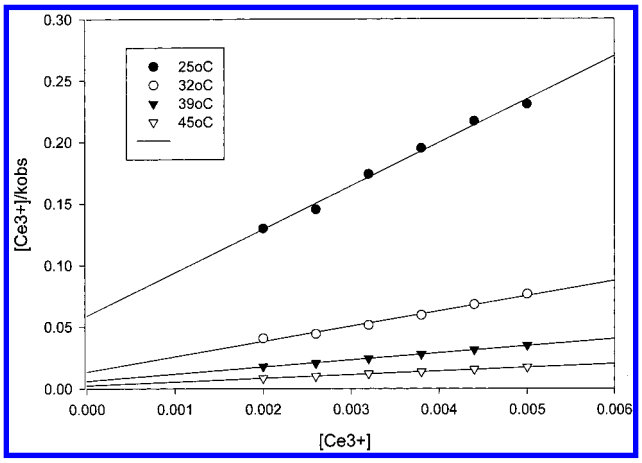

Figure 5. Plot of [Ce^{3+}]/k_{obs} vs [Ce^{3+}] at pH 6.3.

and various solution pH's and initial concentrations of Ce^{3+}. Initial plots (not shown) of k_{obs} vs [Ce^{3+}] show saturation behavior, similar to what has been observed for the Ln−DOTA and Cu^{2+}/Ni^{2+}−TETA formation systems.[7−9,26] Thus, the proposed reaction steps and the rate equation are as follows:

$$Ce^{3+} + H_2TETA^{2-} \overset{K^*}{\longleftrightarrow} Ce(H_2TETA)^{+,*} \xrightarrow[-H^+]{k} Ce(HTETA)^* \xrightarrow[-H^+]{k} CeTETA^-$$

$$k_{obs} = kK^*[Ce^{3+}]/(1 + K^*[Ce^{3+}]) \quad (3)$$

According to eq 3, the plots of [Ce^{3+}]/k_{obs} vs [Ce^{3+}] give values of k (1/slope) and K^* (slope/intercept), the equilibrium constant for the precursor complex formation. Figure 5 shows one example of such a plot at pH 6.3. The obtained k and log K^* values are listed in Table 5.

(26) Kasprzyk, S. P.; Wilkins, R. G. *Inorg. Chem.* **1982**, *21*, 3349−3352.

Table 5. Resolved Rate Constants (k, s^{-1}) for the Formation of Cerium(III)−TETA Complex and the Equilibrium Constant for the Formation of the Intermediate (log K^*, M^{-1}) at pH 6.1−6.7 at Four Different Temperatures, $\mu = 1.0$ (KCl)

		k, s^{-1}			
pH	[OH^-], M	25 °C	32 °C	39 °C	45 °C
6.1	1.73×10^{-8}		0.03293	0.06476	0.15816
6.3	2.75×10^{-8}	0.02867	0.08151	0.17821	0.34180
6.5	4.36×10^{-8}	0.05419	0.14543	0.39897	0.76640
6.7	6.92×10^{-8}	0.11600	0.30150	0.75112	1.33831

	log K^*, M^{-1}			
pH	25 °C	32 °C	39 °C	45 °C
6.1		2.95	2.99	2.97
6.3	2.79	2.95	2.98	3.09
6.5	2.93	2.95	2.80	2.91
6.7	2.78	2.81	2.82	3.10
av	2.92 ± 0.10			

The average log K^* value is 2.92, which is in the range of the formation constants of Ce(III) binding with one (log $K \sim 1.8$) and two (log $K \sim 3.1$) carboxylate ligands,[27] and is smaller than that of Ce(III)−H_2DOTA complex formation[8] (log $K^* = 4.5$, pH 4.8). If it is assumed that the intermediate is Eu(H_2-TETA)$^+$ with the four carboxylates in the syn configuration, it probably means that its formation requires ligand rearrangement and the resulting structure is less stable. This is consistent with the fact that the preorganized H_2DOTA with the four carboxylate arms pointing to the same side forms a more stable intermediate than that of Ce(III)−H_2TETA.

The values of k increase with increasing pH in the small pH range studied. This can be explained as OH^- ion assisted rearrangement of the intermediate,[7−9] and an expression consistent with this observation is given by

$$k = k_{H_2O} + k_{OH}[OH^-] \quad (4)$$

Plots of k vs [OH^-] at each temperature give slope k_{OH} (the rate constant of the mono-hydroxide ion assisted intermediate rearrangement pathway) and intercept k_{H_2O} (the self-rearrangement rate constant) values. Since the intercept values are negative and must be regarded as zero, the plots were redrawn and a second order dependence relationship gives a better fit (Figure 6),

$$k = k_{OH}[OH^-] + k_{2OH}[OH^-]^2 \quad (5)$$

where k_{2OH} represent the rate constant of the di-hydroxide ion assisted intermediate rearrangement pathway. The values of k_{OH} and k_{2OH} are listed in Table 6. Previously, only a mono-hydroxide ion assisted intermediate rearrangement pathway was proposed for the Ln(DOTA)$^-$ formation reaction.[7−9] The presence of the di-hydroxide ion assisted pathway for Ce(TETA)$^-$ formation implies that the nonpreorganized TETA ligand rearrangement could be further accelerated by a second hydroxide ion to form the final Ce(TETA)$^-$ complex. For Ln(DOTA)$^-$ complex formation, Kumar et al. proposed that the more reactive intermediate species was the monoprotonated Ln(HDOTA).[7] However, because of the presence of both mono- and di-hydroxide ion assisted pathway, both Ce(H_2TETA)$^+$ and Ce(HTETA) are reactive species.

(27) Martell, A. E.; Smith, R. M. *Critical Stability Constants*; Plenum: New York, 1977; Vol. 3.

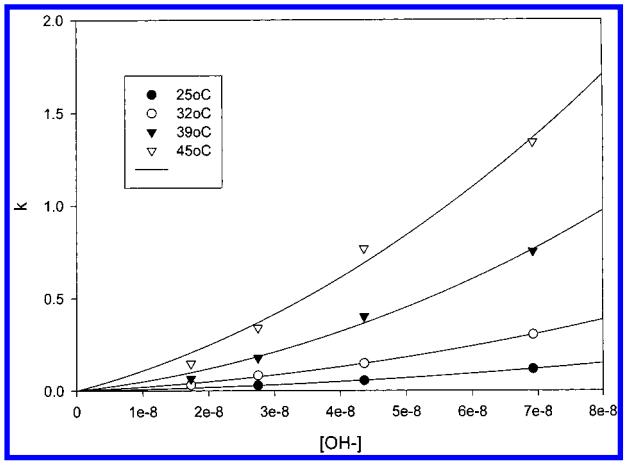

Figure 6. Plots of k vs [OH$^-$] at four different temperatures for the formation of Ce(TETA)$^-$. A second-order dependence relationship gives better fit.

Table 6. The Resolved Rate Constants, k_{OH} (M^{-1} s^{-1}) and k_{2OH} (M^{-2}, s^{-1}) at Various Temperatures

	25 °C	32 °C	39 °C	45 °C
k_{OH}	5.58×10^5	1.60×10^6	3.80×10^6	9.21×10^6
k_{2OH}	1.61×10^{13}	4.00×10^{13}	1.04×10^{14}	1.51×10^{14}

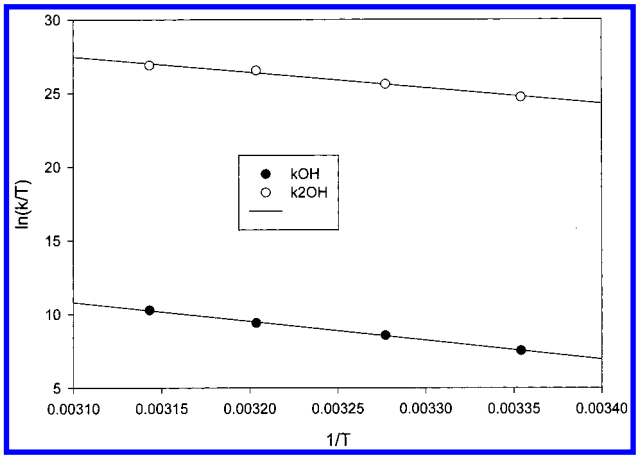

Figure 7. Plots of ln(k/T) vs (1/T) for k_{OH} and k_{2OH} of Ce(TETA)$^-$ formation.

By using the Eyring equation,[28] additional plots of ln(k/T) vs (1/T) yield the following information (T is absolute temperature, K):

$$\ln(k/T) = \ln(k_b/h) - (\Delta H^{\ddagger}/RT) + (\Delta S^{\ddagger}/R) \quad (6)$$

$$\text{slope} = -\Delta H^{\ddagger}/R \quad (7)$$

$$\text{intercept} = (\Delta S^{\ddagger}/R) + \ln(k_b/h) \quad (8)$$

where R is the gas constant (1.98719 cal mol^{-1} K^{-1}), k_b is Boltzmann's constant (1.381×10^{-23} J K^{-1}), and h is Planck's constant (6.626×10^{-34} J s) (Figure 7). The free energy of activation, $\Delta G^{\ddagger}$, can be calculated according to the following equation:

$$\Delta G^{\ddagger} = \Delta H^{\ddagger} - T\Delta S^{\ddagger} \quad (9)$$

Table 7 lists the values of $\Delta H^{\ddagger}$, $\Delta S^{\ddagger}$, and $\Delta G^{\ddagger}$ at 25 °C (298 K).

(28) Espenson, J. H. *Chemical Kinetics and Reaction Mechanisms*; McGraw-Hill Book Co.: New York, 1981.

Table 7. Rate Activation Parameters for the Formation of Ce(TETA)$^-$ and Ce(DOTA)$^-$ Complexes at 25 °C[a]

	Ce(TETA)$^-$		Ce(DOTA)$^-$
	k_{OH}	k_{2OH}	k_{OH}
$\Delta H^{\ddagger}$, kcal/mol	25.47	21.12	18.80
$\Delta S^{\ddagger}$, eu	53.21	72.82	32.23
$\Delta G^{\ddagger}$, kcal/mol	9.61	−0.59	9.19

[a] Ce(DOTA)$^-$ data were estimated from rate data obtained at [Ce^{3+}] = 4.4 mM. See text for details.

Table 8. Observed Rate Constants (k_{obs}, s^{-1}) for the Formation of Cerium(III)−DOTA Complex at pH 6.1−6.7 at Four Different Temperatures, μ = 1.0 (KCl)

		k_{obs}, s^{-1}			
pH	[Ce^{3+}], mM	25 °C	32 °C	39 °C	45 °C
6.1	4.4	0.0168	0.0292	0.0572	0.1500
6.3	4.4	0.0292	0.0691	0.1400	0.2630
6.5	4.4	0.0515	0.1064	0.2180	0.3950
6.7	4.4	0.0820	0.1590	0.3330	0.6320

Table 9. Resolved Rate Constants (k_{OH}, M^{-1} s^{-1}) for the Formation of Ce(DOTA)$^-$ Complex at pH 6.1−6.7 at Four Different Temperatures, [Ce^{3+}] = 4.4 mM, μ = 1.0 (KCl)

	25 °C	32 °C	39 °C	45 °C
k_{OH}	1.164×10^6	2.330×10^6	4.827×10^6	9.139×10^6

The $\Delta H^{\ddagger}$ value is greater for the mono-hydroxide ion assisted pathway. It is also greater than those of many other macrocyclic complexes.[21,22] This indicates that, even with hydroxide ion assistance, lanthanide ion induced TETA ligand conformational rearrangement still requires greater activation enthalpy. The $\Delta H^{\ddagger}$ value is smaller for the di-hydroxide ion assisted pathway, indicating that, when [OH$^-$] is higher, the final complex is easier to form. The positive $\Delta S^{\ddagger}$ values are consistent with the nature of OH$^-$ ion assistance, i.e., the OH$^-$ ion could assist the dissociation of the proton from nitrogen. The deprotonated macrocyclic ligand is also more flexible and results in a greater $\Delta S^{\ddagger}$ value.

For comparison purposes, the pseudo-first-order formation rate constants of Ce(DOTA)$^-$ have been measured at four different temperatures, pH 6.1−6.7, [Ce^{3+}] = 4.4 mM (Table 8). According to eq 3 and assuming that the K^* value is ~1.8 $\times 10^6$ for Ce(H$_2$DOTA)$^+$,[9] the ratio K^*[Ce^{3+}]/(1 + K^*[Ce^{3+}]) on the right-hand side of the equation is roughly 1 and k_{obs} = k. The resolved rate constants, k_{OH}, could then be obtained by fitting the rate data to eq 4 and are listed in Table 9. (All k_{H_2O} values are, as expected, zero.) The estimated activation parameters could then be obtained using the Eyring equation plot, and the values are also listed in Table 7. The estimated $\Delta H^{\ddagger}$ and $\Delta G^{\ddagger}$ values for the mono-OH$^-$ ion assisted pathway of the Ce(DOTA)$^-$ formation reaction are smaller than those of the Ce(TETA)$^-$ system, consistent with the fact that the observed rate constants are greater at lower pH and temperature for Ce(DOTA)$^-$ formation.

In summary, linear ligands such as EDTA and DTPA (non-preorganized) and macrocyclic ligands TETA (non-preorganized) and DOTA (preorganized) represent three different types of ligand structures for lanthanide complex formation. Ln−EDTA/DTPA complex formation is usually much faster among the three. Ln−DOTA complex formation is slower because of the rigid, preorganized ligand strain. Ln−TETA complex formation could be comparable to that of Ln−DOTA but with greater pH and temperature dependence and could be more complex in formation reaction mechanisms, e.g., presence of di-hydroxide ion assisted pathway.

Acknowledgment. We would like to thank the National Science Council for financial support of the present research (NSC 88-2113-M-009-012). Thanks are also due to the Regional Instrument Center for the use of the laser-excited luminescence facilities and Dr. Jyh-Shyong Ho for some helpful discussions.

Supporting Information Available: Figures S1, S2, S3, and S4 showing molecular mechanics calculated structures of H_2DOTA, $Eu(DOTA)^-$, $Eu(TETA)^-$, and $Eu(H_2TETA)^+$. This material is available free of charge via the Internet at http://pubs.acs.org.

IC001325J